Methods

Differential Global Positioning System (DGPS). A DGPS survey was carried out in order to obtain a high resolution digital elevation model of the Kamil Crater area, namely a ca. 800 x 500 m area with the crater at centre. We used the GPS 4000SSI equipment for a reference station. We employed a RTK 5700 instrument to collect topographic data with a <1 cm resolution. The collected data were processed using the GPS Processing Program Trimble Geomatic Office to obtain the coordinates of the investigated area. These coordinates are referenced to the Ellipsoid, the projection used was UTM (Universal Transverse Mercator) Zone 35N, the Datum is WGS 84 (World Geodetic System 1984), and the Geoidal Model is EGM96 (Earth Geopotential Model 1996). Part of the digital elevation model is shown in Fig. 3a.

*Ground Penetrating Radar (GPR)***.** A GPR survey was carried out to obtain stratigraphic information in the Kamil Crater area, with particular attention to the lithological units in the crater. A GSSI (Geophysical Survey System Inc.) Sir 2000 instrument, equipped with 400 and 200 MHz monostatic antennae, was used. GPR measurements were acquired along northwest-southeast and northeast-southwest profiles running through the crater. Time to depth conversion was made by both hyperbola analysis and common midpoint measures (by means of a bistatic 80 MHz antenna). The B-B' radargram was carried out at 400 MHz central frequency along the presumed impactor's trajectory and allowed the recognition of an asymmetric crater floor (Fig. 3b).

Geomagnetic survey. The geomagnetic survey covered an area of ca. 250 x 250 meters, centered on the impact crater. The survey was carried out after systematic searches for meteorites larger than 10 g, in order to explore the possible occurrence of buried masses of the impactor, and mini-to-micro-sized impactor debris. The measurements were taken along north-south profile lines about 1.5 meters apart in the area outside the crater, for a cumulative distance of 38 km and 62000 magnetic stations. The crater area was covered with the rover magnetometer attached to a wire stretched across the rim and it was moved from side to side by pulling ropes. This way the magnetic data were acquired at stations on a nearly flat surface level with the ground outside the crater.

The geomagnetic survey was conducted using a GSM19 Overhauser magnetometer (GEM system, Canada) with integrated internal GPS. The sensor was kept close to the ground surface (about 20 – 30 cm high) to investigate the possible presence of microscopic meteoritic debris. In the meantime, a base station was installed nearby for diurnal correction using a proton precession magnetometer. The data were acquired at a rate of 0.5 seconds for the rover unit, and every 30 seconds at the base station. Data are shown in Fig. 3a.

Systematic search for meteorites. Systematic search for meteorites was conducted by a team of seven persons within a 450 x 450 m area with the crater at centre, which had been subdivided into 50 x 50 m cells to optimize operations. Due to the large amount of meteorites we focused on specimens > ca. 10 g. A total of 3634 shrapnel and one large individual amounting to a total of ca. 1.2 tons were collected within this area. Subsequently, systematic search was conducted along a number of concentric and radial traverses up to 1.7 km from the crater. During this exercise, 1544 meteorite specimens were found, weighed (yielding a total mass of 0.5 tons), and left in the field after recording their positions. Field data allowed us to estimate that search covered 50% of the meteorite-bearing surface, which constrains the total mass of the impactor present in the area in the form of > 10 g specimens to ca. 4 tons. No meteorites were found during long-range (up to 5 km from the crater) surveys.

Systematic search for microscopic magnetic particles. In order to study the distribution of microscopic particles associated with the impactor, the < 5 mm magnetic extract of the soil was sampled along eight radial traverses (one every 45°) extending for up to 1.3 km from the crater rim, at incremental distances. Each sample was obtained from a 30 x 30 x 5 cm soil volume. A total of 44 samples was collected, washed in deionized water and subsequently dry-sieved and weighed prior to petrographic investigation. The concentrations of microscopic particles in 10 representative samples were used to constrain the total mass of the impactor present in the area in the form of microscopic particles to several tons.

Electron Probe Microanalyses (EPMA). The compositions of the mineral phases of the Gebel Kamil meteorite were determined with a CAMECA SX50 electron microprobe with four wavelength-dispersive spectrometers at the CNR Istituto di Geoscienze e Georisorse in Padova. Running conditions were 20 kV accelerating voltage, 20 nA beam current, and 1 µm nominal beam spot. Counting times for the determined elements were 20 s and 10 s at peak and background, respectively. The manufacturer-supplied PAP procedure was employed for raw data reduction. Pure elements and mineral standards were used for instrumental calibration. Selected mineral compositions are reported in Table DR1.

Table DR1. Selected analyses (EPMA) of mineral phases of the Gebel Kamil meteorite.

Analysis #	2	3	37	5	121	124	7	9	20	11	13	28	33	15	25	27	
Mineral	dau	dau	dau	tro	tro	tro	sch	sch	sch	kam	kam	kam	kam	tae	tae	tae	d.l. (wt%)
Si (wt%)	0.02	0.02	< d.l.	0.03	0.02	0.03	0.02	0.02	0.03	0.02	< d.l.	0.03	< d.l.	0.02	0.04	0.02	0.02
P	< d.l.	< d.l.	< d.l.	< d.l.	< d.l.	< d.l.	14.7	14.2	14.7	< d.l.	< d.l.	< d.l.	0.06	< d.l.	< d.l.	< d.l.	0.02
S	43.7	43.9	43.6	36.3	36.1	36.3	< d.l.	0.06	< d.l.	< d.l.	< d.l.	< d.l.	< d.l.	< d.l.	< d.l.	< d.l.	0.06
Cr	35.6	35.9	35.8	0.19	0.18	0.25	< d.l.	< d.l.	< d.l.	< d.l.	< d.l.	< d.l.	< d.l.	< d.l.	< d.l.	< d.l.	0.06
Mn	0.08	0.08	0.08	< d.l.	< d.l.	< d.l.	< d.l.	< d.l.	< d.l.	< d.l.	< d.l.	< d.l.	< d.l.	< d.l.	< d.l.	0.04	0.04
Fe	19.3	19.1	19.2	63.3	63.1	63.2	50.0	50.2	32.1	94.6	93.7	93.5	93.9	66.6	66.5	68.2	0.06
Co	< d.l.	< d.l.	< d.l.	< d.l.	< d.l.	< d.l.	0.18	0.17	0.07	1.12	1.10	1.00	1.08	0.36	0.34	0.36	0.06
Ni	< d.l.	< d.l.	0.08	< d.l.	< d.l.	< d.l.	34.1	34.8	51.9	5.2	5.79	4.76	5.04	32.9	33.3	31.1	0.06
Total	98.6	99.0	98.8	99.8	99.3	99.7	99.0	99.9	98.8	100.9	100.6	99.3	100.1	99.9	100.2	99.8	
Cation formula (a.p.f.u.)																	
Si	0.002	0.002		0.001	0.001	0.001	0.002	0.001	0.002	0.000		0.001		0.000	0.001	0.000	
P							0.972	0.964	0.981				0.001				
S	3.982	3.989	3.974	0.996	0.996	0.998		0.004									
Cr	2.001	2.010	2.012	0.003	0.003	0.004											
Mn	0.004	0.004	0.004													0.000	
Fe	1.009	0.994	1.005	0.999	1.000	0.997	1.830	1.822	1.188	0.939	0.934	0.944	0.940	0.678	0.674	0.694	
Co							0.006	0.006	0.002	0.010	0.010	0.010	0.010	0.003	0.003	0.003	
Ni			0.004				1.188	1.203	1.824	0.049	0.055	0.046	0.048	0.318	0.321	0.301	
∑ Atoms	7	7	7	2	2	2	4	4	4	1	1	1	1	1	1	1	

Abbreviations: dau, daubréelite; tro, troilite; sch, schreibersite; kam, kamacite; tae, taenite; d.l., detection limit.

Figure DR1 . Field photos of the Kamil Crater (Egypt). A: The southern wall of the crater shows upturned bedding of the bedrock. The top of the crater fill unit consisting of fallback debris is shown, along with part of the aeolian sand deposit covering the crater floor. B: An ejecta ray (mainly pale sandstone blocks and boulders) emanating from the crater rim (the ejection direction to the SSE is arrowed). C: Overturned bedrock at the rim crest. D: Landing site of a jet of shrapnel.

Figure DR2. Field photos of prehistoric structures in the Kamil Crater area. A: Ejecta (pale sandstone blocks) overlying a prehistoric trail ~200 m due north of the Kamil Crater. B: Ruins of one of the prehistoric settlements found within 1 km from the Kamil Crater. A number of tools made from local, terrestrial rocks were found therein (inset: mortar at left and a sharpener on the right; both about 20 cm in diameter), but no artifacts worked from meteoritic iron.

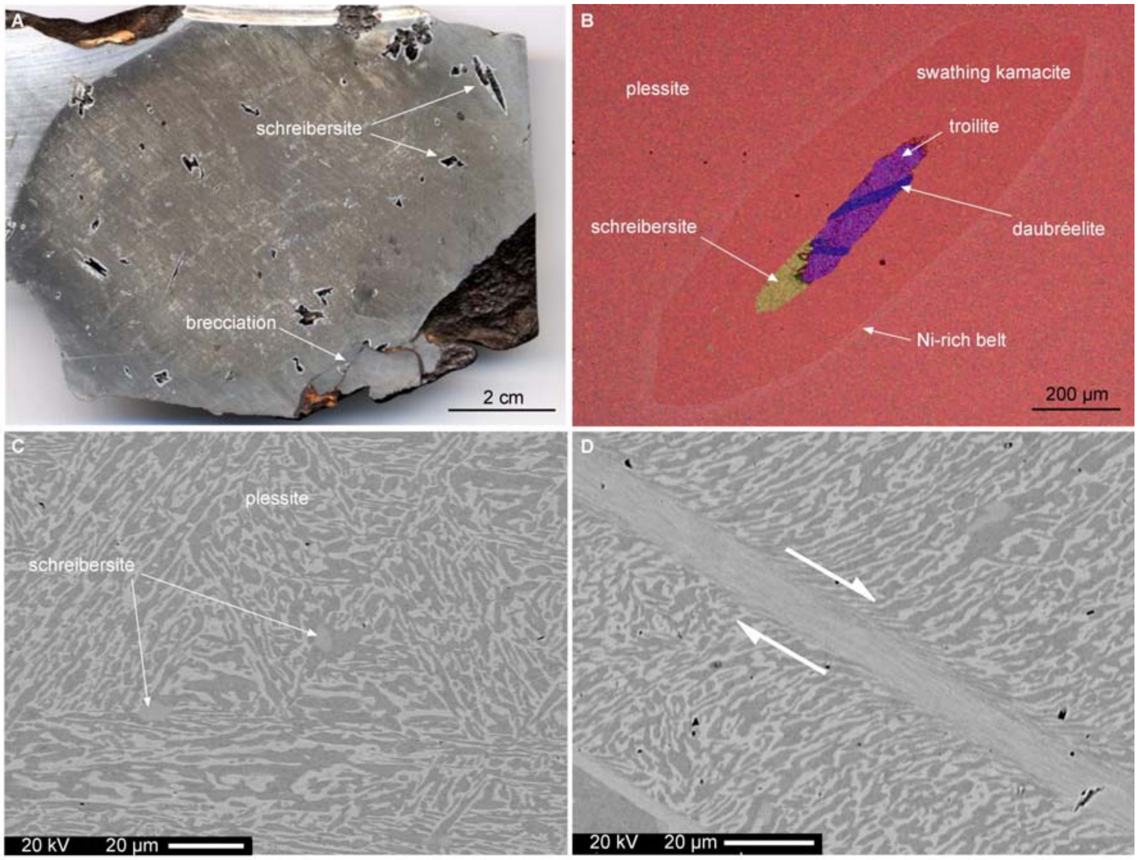

Figure DR3 . Selected petrographic images of a piece of shrapnel of the Gebel Kamil meteorite (A, stereomicrograph; B, composite X-ray elemental map, C-D, back scattered electron images); see also Fig. 2. A: A polished and etched internal surface showing ataxitic texture speckled with schreibersite inclusions. B: A mineral cluster consisting of a schreibersite, troilite and daubréelite association surrounded by swathing kamacite, set in a matrix of duplex plessite. C: A detail of the duplex plessite given by fine intergrowth of kamacite (dark grey) and taenite (pale gray) arranged in a micro-Widmanstätten pattern. D: A microscopic shear band attesting to the high stress associated with the impact.